Nonequilibrium spin glass dynamics from picoseconds to 0.1 seconds

F. Belletti,[1] M. Cotallo,[2] A. Cruz,[3,2] L.A. Fernandez,[4,2] A. Gordillo-Guerrero,[5,2] M. Guidetti,[1] A. Maiorano,[1,2] F. Mantovani,[1] E. Marinari,[6] V. Martin-Mayor,[4,2] A. Muñoz Sudupe,[4] D. Navarro,[7] G. Parisi,[6] S. Perez-Gaviro,[2] J. J. Ruiz-Lorenzo,[5,2] S.F. Schifano,[1] D. Sciretti,[2] A. Tarancon,[3,2] R. Tripiccione,[1] J.L. Velasco,[2] and D. Yllanes[4,2]

[1]*Dipartimento di Fisica Università di Ferrara and INFN - Sezione di Ferrara, Ferrara, Italy.*
[2]*Instituto de Biocomputación y Física de Sistemas Complejos (BIFI), Zaragoza, Spain.*
[3]*Departamento de Física Teórica, Universidad de Zaragoza, 50009 Zaragoza, Spain.*
[4]*Departamento de Física Teórica I, Universidad Complutense, 28040 Madrid, Spain.*
[5]*Departamento de Física, Universidad de Extremadura, 06071 Badajoz, Spain.*
[6]*Dipartimento di Fisica, INFM and INFN, Università di Roma "La Sapienza", 00185 Roma, Italy.*
[7]*Departamento de Ingeniería, Electrónica y Comunicaciones and Instituto de Investigación en Ingeniería de Aragón, Universidad de Zaragoza, 50018 Zaragoza, Spain.*

(Dated: September 5, 2008)

We study numerically the nonequilibrium dynamics of the Ising Spin Glass, for a time that spans eleven orders of magnitude, thus approaching the experimentally relevant scale (i.e. *seconds*). We introduce novel analysis techniques that allow to compute the coherence length in a model-independent way. Besides, we present strong evidence for a replicon correlator and for overlap equivalence. The emerging picture is compatible with non-coarsening behavior.

PACS numbers: 75.50.Lk, 75.40.Gb, 75.40.Mg

Spin Glasses[1] (SG) exhibit remarkable features, including slow dynamics and a complex space of states: their understanding is a key problem in condensed-matter physics that enjoys a paradigmatic status because of its many applications to glassy behavior, optimization, biology, financial markets, social dynamics.

Experiments on Spin Glasses[1, 2] focus on nonequilibrium dynamics. In the simplest experimental protocol, isothermal aging hereafter, the SG is cooled as fast as possible to the working temperature below the critical one, $T < T_c$. It is let to equilibrate for a *waiting time*, t_w. Its properties are probed at a later time, $t + t_w$. The thermoremanent magnetization is found to be a function of t/t_w, for $10^{-3} < t/t_w < 10$ and t_w in the range 50 s — 10^4 s[3] (see, however,[4]). This lack of any characteristic time scale is named *Full-Aging*. Also the growing size of the coherent domains, the coherence-length, ξ, can be measured[5, 6]. Two features emerge: (i) the lower T is, the slower the growth of $\xi(t_w)$ and (ii) $\xi \sim 100$ lattice spacings, even for $T \sim T_c$ and $t_w \sim 10^4$ s[5].

The sluggish dynamics arises from a thermodynamic transition at T_c[7, 8, 9]. There is a sustained theoretical controversy on the properties of the (unreachable in human times) equilibrium low temperature SG phase, which is nevertheless relevant to (basically nonequilibrium) experiments[10]. The main scenarios are the droplets[11], replica symmetry breaking (RSB)[12], and the intermediate Trivial-Non-Trivial (TNT) picture[13].

Droplets expects two equilibrium states related by global spin reversal. The SG order parameter, the spin overlap q, takes only two values $q = \pm q_{EA}$. In the RSB scenario an infinite number of pure states influence the dynamics[12, 14, 15], so that all $-q_{EA} \leq q \leq q_{EA}$ are reachable. TNT[13] describes the SG phase similarly to an antiferromagnet with random boundary conditions: even if q behaves as for RSB systems, TNT agrees with droplets in the vanishing surface-to-volume ratio of the largest thermally activated spin domains (i.e. the link-overlap defined below takes a single value).

Droplets isothermal aging[16] is that of a disguised ferromagnet[36]. A picture of isothermal aging emerges that applies to basically all coarsening systems: superuniversality[16]. For $T < T_c$ the dynamics consists in the growth of compact domains (inside which the spin overlap coherently takes one of its possible values $q = \pm q_{EA}$). Time dependencies are entirely encoded in the growth law of these domains, $\xi(t)$. The antiferromagnet analogy suggests a similar TNT Aging behavior.

Since in the RSB scenario $q = 0$ equilibrium states do exist, the nonequilibrium dynamics starts, and remains forever, with a vanishing order parameter. The replicon, a critical mode analogous to magnons in Heisenberg ferromagnets, is present for all $T < T_c$[17]. Furthermore, q is not a privileged observable (overlap equivalence[14]): the link overlap displays equivalent Aging behavior.

These theories need numerics to be quantitative[18, 19, 20, 21, 22, 23, 24, 25, 26], but simulations are too short: one Monte Carlo Step (MCS) corresponds to 10^{-12} s[1]. The experimental scale is at 10^{14} MCS (~ 100 s), while typical nonequilibrium simulations reach $\sim 10^{-5}$s. In fact, high-performance computers have been designed for SG simulations[27, 28, 29].

Here we present the results of a large simulation campaign performed on the application-oriented Janus computer [29]. Janus allows us to simulate the SG instantaneous quench protocol for 10^{11} MCS ($\sim$0.1 s), enough to reach experimental times by mild extrapolations. Aging is investigated both as a function of time and temper-

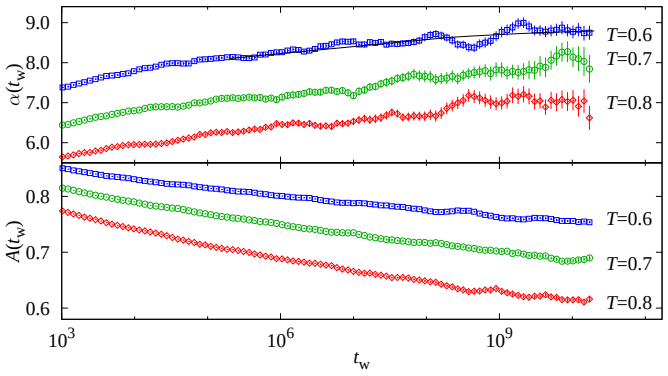

FIG. 1: (Color online) Fit parameters, A and α ($C(t,t_{\rm w}) = A(t_{\rm w})(1+t/t_{\rm w})^{-1/\alpha(t_{\rm w})}$) vs. $t_{\rm w}$ for temperatures below $T_{\rm c}$ ($T=0.6$ line: fit (for $t_w > 10^5$) to $\alpha(t_{\rm w}) = \alpha_0 + \alpha_1 \log t_{\rm w} + \alpha_2 \log^2 t_{\rm w}$, $\alpha_0 = 6.35795$, $\alpha_1 = 0.18605$, $\alpha_2 = -0.00351835$, diagonal $\chi^2/{\rm dof} = 66.26/63$). Coherent oscillations are due to the strong correlations of $\alpha(t_{\rm w})$ at neighboring times (neither statistical errors nor the fitting curve nor $\chi^2/{\rm dof}$ vary if one bins data in blocks of 5 consecutive $t_{\rm w}$).

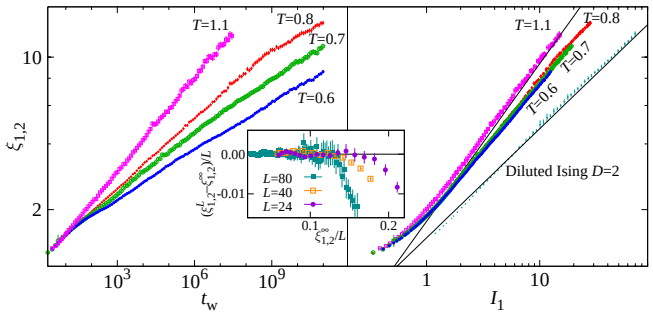

FIG. 2: (Color online) **Left:** SG coherence length $\xi_{1,2}$ vs. waiting time, for $T \le T_{\rm c}$. **Right:** $\xi_{1,2}$ vs. I_1, ($\xi_{1,2} \propto I_1^{1/(2-a)}$). Also shown data for the 2-D site-diluted Ising model ($L=4096$, 25% dilution, average over 20 samples, $T = 0.64 T_{\rm c}^{\rm Ising}$, $\xi_{1,2}$ and I_1 rescaled by 2 for clarity). Full lines correspond to Ising $a=0$, (coarsening) and to the SG, $a(T_{\rm c}) = 0.616$[30]. **Inset:** $[\xi^L_{1,2}(t_{\rm w}) - \xi^\infty_{1,2}(t_{\rm w})]/L$ vs. $\xi^\infty_{1,2}(t_{\rm w})/L$ for $T=0.8$ and $L = 24, 40$ and 80 ($\xi^\infty_{1,2}(t_{\rm w})$ from a fit $\xi_{1,2}(t_{\rm w}) = A(T) t_{\rm w}^{1/z(T)}$ for $L=80$ in the range $3 < \xi_{1,2} < 10$, see text).

ature. We obtain model-independent determinations of the SG coherence length ξ. Conclusive evidence is presented for a critical correlator associated with the replicon mode. We observe non trivial Aging in the link correlation (a *nonequilibrium* test of overlap equivalence[14]). We conclude that, up to experimental scales, SG dynamics is not coarsening like.

The $D=3$ Edwards-Anderson Hamiltonian is

$$\mathcal{H} = -\sum_{\langle \boldsymbol{x},\boldsymbol{y}\rangle} J_{\boldsymbol{x},\boldsymbol{y}} \sigma_{\boldsymbol{x}}\, \sigma_{\boldsymbol{y}}\,, \quad (\langle \dots \rangle : \text{nearest neighbors})\,. \quad (1)$$

The spins $\sigma_{\boldsymbol{x}} = \pm 1$ are placed on the nodes, $\boldsymbol{x}$, of a cubic lattice of linear size L and periodic boundary conditions. The couplings $J_{\boldsymbol{x},\boldsymbol{y}} = \pm 1$ are chosen randomly with 50% probability, and are quenched variables. For each choice of the couplings (one sample), we simulate two independent systems, $\{\sigma^{(1)}_{\boldsymbol{x}}\}$ and $\{\sigma^{(2)}_{\boldsymbol{x}}\}$. We denote by $\overline{(\cdots)}$ the average over the couplings. Model (1) undergoes a SG transition at $T_{\rm c} = 1.101(5)$[30].

Our $L = 80$ systems evolve with a Heat-Bath dynamics[31], which is in the Universality Class of the physical evolution. The fully disordered starting spin configurations are instantaneously placed at the working temperature (96 samples at $T = 0.8 \approx 0.73\, T_{\rm c}$, 64 at $T = 0.7 \approx 0.64\, T_{\rm c}$ and 96 at $T = 0.6 \approx 0.54\, T_{\rm c}$). We also perform shorter simulations (32 samples) at $T_{\rm c}$, as well as $L=40$ and $L=24$ runs to check for Finite-Size effects.

A crucial quantity in non equilibrium dynamics is the two-times correlation function (defined in terms of the field $c_{\boldsymbol{x}}(t,t_{\rm w}) \equiv \sigma_{\boldsymbol{x}}(t+t_{\rm w})\sigma_{\boldsymbol{x}}(t_{\rm w})$)[18, 19, 22]:

$$C(t,t_{\rm w}) = \overline{L^{-3}\sum_{\boldsymbol{x}} c_{\boldsymbol{x}}(t,t_{\rm w})}\,, \quad (2)$$

linearly related to the real part of the a.c. susceptibility at waiting time $t_{\rm w}$ and frequency $\omega = \pi/t$.

To check for Full-Aging[3] in a systematic way, we fit $C(t,t_{\rm w})$ as $A(t_{\rm w})(1+t/t_{\rm w})^{-1/\alpha(t_{\rm w})}$ in the range $t_{\rm w} \le t \le 10 t_{\rm w}$ [37], obtaining fair fits for all $t_{\rm w} > 10^3$. To be consistent with the experimental claim of Full-Aging behavior for $10^{14} < t_{\rm w} < 10^{16}$[3], $\alpha(t_{\rm w})$ should be constant in this $t_{\rm w}$ range. Although $\alpha(t_{\rm w})$ keeps growing for our largest times (with the large errors in[22] it seemed constant for $t_{\rm w} > 10^4$), its growth slows down. The behavior at $t_{\rm w} = 10^{16}$ seems beyond reasonable extrapolation.

The coherence length is studied from the correlations of the replica field $q_{\boldsymbol{x}}(t_{\rm w}) \equiv \sigma^{(1)}_{\boldsymbol{x}}(t_{\rm w})\sigma^{(2)}_{\boldsymbol{x}}(t_{\rm w})$,

$$C_4(\boldsymbol{r},t_{\rm w}) = \overline{L^{-3}\sum_{\boldsymbol{x}} q_{\boldsymbol{x}}(t_{\rm w}) q_{\boldsymbol{x}+\boldsymbol{r}}(t_{\rm w})}\,. \quad (3)$$

For $T < T_{\rm c}$, it is well described by[12, 20]

$$C_4(\boldsymbol{r},t_{\rm w}) \sim r^{-a} {\rm e}^{-(r/\xi(t_{\rm w}))^b}, \quad a \simeq 0.5,\ b \simeq 1.5\,. \quad (4)$$

The actual value of a is relevant. For coarsening dynamics $a=0$, while in a RSB scenario $a > 0$ and $C_4(r,t_{\rm w})$ vanishes at long times for fixed $r/\xi(t_{\rm w})$. At $T_{\rm c}$, the latest estimate is $a = 1+\eta = 0.616(9)$ [30].

To study a independently of a particular Ansatz as (4) we consider the integrals

$$I_k(t_{\rm w}) = \int_0^\infty {\rm d}r\, r^k C_4(r,t_{\rm w})\,, \quad (5)$$

(e.g. the SG susceptibility is $\chi^{\rm SG}(t_{\rm w}) = 4\pi I_2(t_{\rm w})$). As we assume $L \gg \xi(t_{\rm w})$ we safely reduce the upper limit to $L/2$. If a scaling form $C_4(r,t_{\rm w}) \sim r^{-a} f(r/\xi(t_{\rm w}))$ is adequate at large r, then $I_k(t_{\rm w}) \propto [\xi(t_{\rm w})]^{k+1-a}$. It follows that $\xi_{k,k+1}(t_{\rm w}) \equiv I_{k+1}(t_{\rm w})/I_k(t_{\rm w})$ is proportional to $\xi(t_{\rm w})$ and $I_1(t_{\rm w}) \propto \xi_{k,k+1}^{2-a}$. We find $\xi^{(2)}(t_{\rm w}) \approx 0.8\, \xi_{1,2}(t_{\rm w})$, where $\xi^{(2)}$ is the noisy second-moment estimate[9]. Furthermore, for $\xi_{1,2} > 3$, we find $\xi_{0,1}(t_{\rm w}) \approx 0.46\, \xi_{1,2}(t_{\rm w})$, and $\xi^{\rm fit}(t_{\rm w}) = 1.06\, \xi_{1,2}(t_{\rm w})$, ($\xi^{\rm fit}$ from a fit to (4) with $a=0.4$).

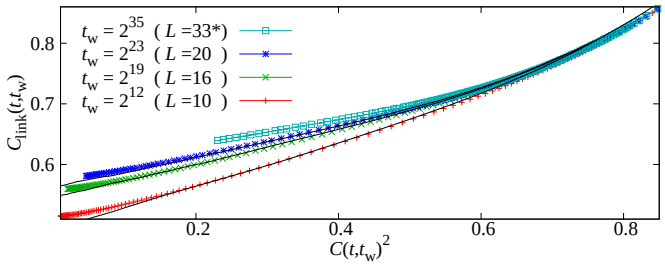

FIG. 3: (Color online) For appropriate t_w and L, the nonequilibrium $C_{link}(t,t_w)$ vs. $C^2(t,t_w)$ at $T=0.7$, coincides with equilibrium $Q_{link}|_q$ vs. q^2 (full lines, data from[34], see text for definitions). The length-time dictionary is $L=10$ or $t_w=2^{12}$, $L=16$ or $t_w=2^{19}$ and $L=20$ or $t_w=2^{23}$. The coherence lengths, $\xi(2^{12})=2.75(3)$, $\xi(2^{19})=4.23(4)$ and $\xi(2^{23})=5.40(7)$, are in the ratio 10:16:20. Hence, from $\xi(2^{35})$, Fig. 2, we predict the equilibrium curve for $L=33$.

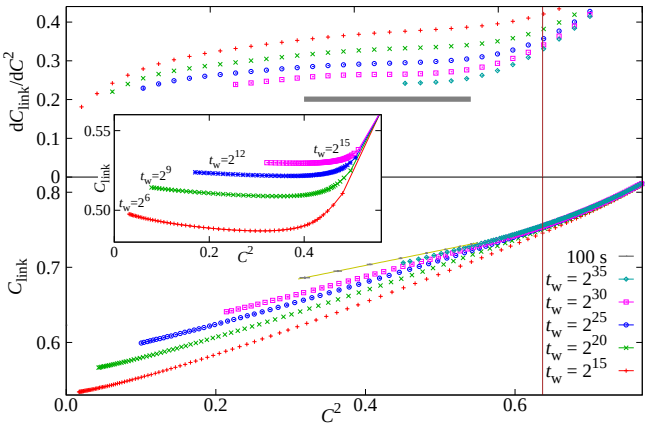

FIG. 4: (Color online) **Bottom:** $C_{link}(t,t_w)$ vs. $C^2(t,t_w)$ for $T=0.6$ and some of our largest t_w (vertical line: q^2_{EA} from[23]). We also show our extrapolation of the C_{link} vs. C^2 curve to $t_w=10^{14}$ (~ 100 s, see text). **Top:** Derivative of C_{link} with respect to C^2 for $T=0.6$. The horizontal line corresponds to the slope of a linear fit of $t_w=10^{14}$ extrapolations (the line width equals twice the error). **Inset:** As in bottom panel, for the ferromagnetic site-diluted $D=2$ Ising model (same simulation of Fig. 2).

Note that, when $\xi \ll L$, irrelevant distances $r \gg \xi$ largely increase statistical errors for I_k. Fortunately, the very same problem was encountered in the analysis of correlated time series[32], and we may borrow the cure[38].

The largest t_w where $L=80$ still represents $L=\infty$ physics follows from Finite Size Scaling[31]: for a given numerical accuracy, one should have $L \geq k\,\xi_{1,2}(t_w)$. To compute k, we compare $\xi^L_{1,2}$ for $L=24, 40$ and 80 with $\xi^\infty_{1,2}$ estimated with the power law described below (Fig. 2—inset). It is clear that the safe range is $L \geq 7\,\xi_{1,2}(t_w)$ at $T=0.8$ (at T_c the safety bound is $L \geq 6\,\xi_{1,2}(t_w)$).

Our results for $\xi_{1,2}$ are shown in Fig. 2. Note for $T=0.8$ the Finite-Size change of regime at $t_w=10^9$ ($\xi_{1,2}\sim 11$). We find fair fits to $\xi(t_w)=A(T)t_w^{1/z(T)}$: $z(T_c)=6.86(16)$, $z(0.8)=9.42(15)$, $z(0.7)=11.8(2)$ and $z(0.6)=14.1(3)$, in good agreement with previous numerical and experimental findings $z(T)=z(T_c)\,T_c/T$[5, 20]. We restricted the fitting range to $3 \leq \xi \leq 10$, to avoid both Finite-Size and lattice discretization effects. Extrapolating to experimental times ($t_w=10^{14}\sim 100$ s), we find $\xi=14.0(3), 21.2(6), 37.0(14)$ and $119(9)$ for $T=0.6$, $T=0.7$, $T=0.8$ and $T=1.1\approx T_c$, respectively, which seem fairly sensible compared with experimental data[5, 6].

In Fig. 2, we also explore the scaling of I_1 as a function of $\xi_{1,2}$ ($I_1 \propto \xi^{2-a}$). The nonequilibrium data for $T=1.1$ scales with $a=0.585(12)$. The deviation from the *equilibrium* estimate $a=0.616(9)$[30] is at the limit of statistical significance (if present, it would be due to scaling corrections). For $T=0.8, 0.7$ and 0.6, we find $a=0.442(11), 0.355(15)$ and $0.359(13)$ respectively (the residual T dependence is probably due to critical effects still felt at $T=0.8$). Note that ground state computations for $L \leq 14$ yielded $a(T=0) \approx 0.4$[33]. These numbers differ both from critical and coarsening dynamics ($a=0$).

We finally address the aging properties of $C_{link}(t,t_w)$

$$C_{link}(t,t_w) = \overline{\sum_{\langle \boldsymbol{x},\boldsymbol{y}\rangle} c_{\boldsymbol{x}}(t,t_w)c_{\boldsymbol{y}}(t,t_w)}/(3L^3)\,. \qquad (6)$$

Experimentalists have yet to find a way to access C_{link}, which is complementary to $C(t,t_w)$ (it does not vanish if the configurations at $t+t_w$ and t_w differ by the spin inversion of a compact region of half the system size).

It is illuminating to eliminate t as independent variable in favor of $C^2(t,t_w)$, Figs. 3 and 4. Our expectation for a coarsening dynamics is that, for $C^2 < q^2_{EA}$ and large t_w, C_{link} will be C-independent (the relevant system excitations are the spin-reversal of compact droplets not affecting C_{link}). Conversely, in a RSB system new states are continuously found as time goes by, so we expect a non constant C^2 dependence even if $C < q_{EA}$ [39].

General arguments tell us that the nonequilibrium C_{link} at finite *times* coincides with equilibrium correlation functions for systems of finite *size*[10], Fig. 3 (Q_{link} is just $C_4(r=1)$, while q is the spatial average of $q_{\boldsymbol{x}}$, Eq.(3)). Therefore, see caption to Fig. 3, we predict the q^2 dependency of the *equilibrium* conditional expectation $Q_{link}|_q$ for lattices as large as $L=33$.

As for the shape of the curve $C_{link} = f(C^2, t_w)$, Fig. 4—bottom, the t_w dependency is residual. Within our time window, C_{link} is not constant for $C < q_{EA}$. For comparison (inset) we show the, qualitatively different, curves for a coarsening dynamics. Therefore, a major difference between a coarsening and a SG dynamics is in the derivative dC_{link}/dC^2, for $C^2 < q^2_{EA}$, Fig. 4—top. We first smooth the curves by fitting $C_{link} = f(C^2)$ to the lowest order polynomial that provides a fair fit (seventh order for $t_w \leq 2^{25}$, sixth for larger t_w), whose derivative was taken afterwards (Jackknife's statistical errors).

Furthermore, we have extrapolated both $C_{link}(t = rt_w, t_w)$ and $C(t = rt_w, t_w)$ to $t_w \approx 10^{14}$ (~ 100 s), for

$r = 8, 4, \ldots, \frac{1}{16}$[40]. The extrapolated points for $t_{\rm w} = 10^{14}$ fall on a straight line whose slope is plotted in the upper panel (thick line). The derivative is non vanishing for $C^2 < q^2_{\rm EA}$, for the experimental time scale.

In summary, Janus[29] halves the (logarithmic) time-gap between simulations and nonequilibrium Spin Glass experiments. We analyzed the simplest temperature quench, finding numerical evidence for a non-coarsening dynamics, at least up to experimental times (see also[26]). Let us highlight: *nonequilibrium* overlap equivalence (Figs. 3,4); nonequilibrium scaling functions reproducing *equilibrium* conditional expectations in finite systems (Fig. 3); and a nonequilibrium replicon exponent compatible with equilibrium computations[33]. The growth of the coherence length sensibly extrapolates to $t_w = 100$ s (our analysis of dynamic heterogeneities[25, 26] will appear elsewhere[35]). Exploring with Janus nonequilibrium dynamics up to the *seconds* scale will allow the investigation of many intriguing experiments.

We corresponded with M. Hasenbusch, A. Pelissetto and E. Vicari. Janus was supported by EU FEDER funds (UNZA05-33-003, MEC-DGA, Spain), and developed in collaboration with ETHlab. We were partially supported by MEC (Spain), through contracts No. FIS2006-08533, FIS2007-60977, FPA2004-02602, TEC2007-64188; by CAM (Spain) and the Microsoft Prize 2007.

[1] J. A. Mydosh, *Spin Glasses: an Experimental Introduction* (Taylor and Francis, London 1993).
[2] E. Vincent et al., in *Complex Behavior of Complex Systems*, Lecture Notes in Physics **492**.
[3] G.F. Rodriguez, G.G. Kenning, and R. Orbach, Phys. Rev. Lett. **91**, 037203 (2003).
[4] V. Dupuis et al., Pramana J. of Phys. **64**, 1109 (2005).
[5] Y. G. Joh et al., Phys. Rev. Lett. **82**, 438 (1999).
[6] F. Bert et al., Phys. Rev. Lett. **92**, 167203 (2004).
[7] K. Gunnarsson et al., Phys. Rev. B **43**, 8199 (1991).
[8] M. Palassini and S. Caracciolo, Phys. Rev. Lett. **82**, 5128 (1999).
[9] H. G. Ballesteros et al., Phys. Rev. B **62**, 14237 (2000).
[10] S. Franz, M. Mézard, G. Parisi, and L. Peliti, Phys. Rev. Lett. **81**, 1758 (1998); J. Stat. Phys. **97**, 459 (1999).
[11] W. L. McMillan, J. Phys. C **17**, 3179 (1984); A. J. Bray, M. A. Moore, in *Heidelberg Colloquium on Glassy Dynamics*, Lecture Notes in Physics **275**; J. L. van Hemmen and I. Morgenstern (ed. Springer, Berlin). D. S. Fisher, D. A. Huse, Phys. Rev. Lett. **56**, 1601 (1986) and Phys. Rev. B **38**, 386 (1988).
[12] E. Marinari et al., J. Stat. Phys. **98**, 973 (2000).
[13] F. Krzakala and O. C. Martin, Phys. Rev. Lett. **85**, 3013 (2000); M. Palassini and A.P.Young, Phys. Rev. Lett. **85**, 3017 (2000).
[14] G. Parisi and F. Ricci-Tersenghi, J. Phys. A: Math. Gen. **33**, 113 (2000).
[15] P. Contucci and C. Giardina, J. Stat. Phys. **126**, 917 (2007); Ann. Henri Poincare **6**, 915 (2005).
[16] D. S. Fisher and D. A. Huse, Phys. Rev. B **38**, 373 (1988).
[17] C. De Dominicis, I. Kondor, and T. Temesvári, in *Spin Glasses and Random Fields*, edited by P. Young, World Scientific (Singapore 1997).
[18] J. Kisker, L. Santen, M. Schreckenberg, and H. Rieger, Phys. Rev. B **53**, 6418 (1996).
[19] H. Rieger, J. Phys. A **26**, L615 (1993).
[20] E. Marinari, G. Parisi, F. Ricci-Tersenghi, and J. J. Ruiz-Lorenzo, J. Phys. A **33**, 2373 (2000).
[21] L. Berthier and J.-P. Bouchaud, Phys. Rev. B **66**, 054404 (2002).
[22] S. Jimenez, V. Martin-Mayor, G. Parisi, and A. Tarancón, J. Phys. A: Math. and Gen. **36**, 10755 (2003).
[23] S. Perez Gaviro, J.J. Ruiz-Lorenzo, and A. Tarancón, J. Phys. A: Math. Gen. **39** (2006) 8567-8577.
[24] S. Jimenez, V. Martin-Mayor, and S. Perez-Gaviro, Phys. Rev. B **72**, 054417 (2005).
[25] L.C. Jaubert, C. Chamon, L.F. Cugliandolo, and M. Picco, J. Stat. Mech. (2007) P05001; H.E. Castillo, C. Chamon, L.F. Cugliandolo, and M.P. Kennett, Phys. Rev. Lett. **88**, 237201 (2002); H.E. Castillo et al., Phys. Rev. B **68**, 134442 (2003).
[26] C. Aron, C. Chamon, L.F. Cugliandolo, M. Picco, J. Stat. Mech. P05016, (2008).
[27] A. Cruz et al., Comp. Phys. Comm. **133**, 165 (2001).
[28] A. Ogielski, Phys. Rev. B **32**, 7384 (1985).
[29] F. Belletti et al., Computing in Science & Engineering **8**, 41-49 (2006); Comp. Phys. Comm. 178, 208 (2008); preprint arXiv:0710.3535.
[30] M. Hasenbusch, A. Pelissetto, and E. Vicari, J. Stat. Mech. L02001 (2008) and private communication.
[31] See, e.g., D. J. Amit and V. Martin-Mayor, *Field Theory, the Renormalization Group and Critical Phenomena,* (World-Scientific Singapore, third edition, 2005).
[32] See e.g. A.D. Sokal, in *Functional Integration: Basics and Applications* (1996 Cargèse school), ed. C. DeWitt-Morette, P. Cartier, and A. Folacci (Plenum, N.Y., 1997).
[33] E. Marinari and G. Parisi, Phys. Rev. Lett. **86**, 3887 (2001).
[34] P. Contucci et al., Phys. Rev. Lett. **99**, 057206 (2007); P. Contucci, C. Giardina, C. Giberti, and C. Vernia, Phys. Rev. Lett. **96**, 217204 (2006).
[35] The Janus collaboration (manuscript in preparation).
[36] Temperature chaos could spoil the analogy if temperature is varied during the Aging experiment[16].
[37] Because data at different t and $t_{\rm w}$ are exceedingly correlated, for all fits in this work we consider the diagonal χ^2 (i.e. we keep only the diagonal terms in the covariance matrix). The effect of time correlations is considered by first forming jackknife blocks[31] (JKB) with the data for different samples (JKB at different t and $t_{\rm w}$ preserve time correlations), then minimizing χ^2 for each JKB[22].
[38] We numerically integrate $C_4(r, t_{\rm w})$ up to a $t_{\rm w}$ dependent cutoff, chosen as the smallest integer such that $C_4(r^{\rm cutoff}(t_{\rm w}), t_{\rm w})$ was smaller than three times its own statistical error. We estimate the (small) remaining contribution, by fitting to Eq.(4) then integrating numerically the fitted function from $r^{\rm cutoff}$–1 to $L/2$. Details (including consistency checks) will be given elsewhere[35].
[39] $C_{\rm link}$=C^2 in the full-RSB Sherrington-Kirkpatrick model.
[40] For each r, both the link and the spin correlation functions are independently fitted to $a_r + b_r t_{\rm w}^{-c_r}$ (fits are stable for $t_{\rm w} > 10^5$ with $c_r \approx 0.5$). These fits are then used to extrapolate the two correlation functions to $t_{\rm w} = 10^{14}$.